

# Effect of Imidization Conditions on the Morphology of Polyimide

Jiann-Wen Huang,<sup>1</sup> Chiun-Chia Kang<sup>2</sup>

<sup>1</sup>General Education Center, Tainan Woman's College of Arts & Technology, 529 Chung Chen Road, Yung Kang City 710, Taiwan, Republic of China

<sup>2</sup>R&D Center, Taroko International Company, Ltd., 473 Jong Shan South Road, Yung Kang City 710, Taiwan, Republic of China

Received 5 June 2003; accepted 2 February 2004

DOI 10.1002/app.20493

Published online in Wiley InterScience (www.interscience.wiley.com).

**ABSTRACT:** A poly(amic acid) derived from pyromellitic dianhydride and oxydianiline was imidized under different conditions. The sample imidized in solution (PI-1) showed the X-ray diffraction pattern of a crystalline material, whereas that of the sample imidized in the solid state was essentially amorphous. Both samples were further characterized by <sup>13</sup>C-NMR spectroscopy, IR spectroscopy, electron

paramagnetic resonance, and thermogravimetric analysis. The orders of polyimide in both the crystalline and amorphous states are discussed. © 2004 Wiley Periodicals, Inc. *J Appl Polym Sci* 93: 1065–1070, 2004

**Key words:** polyimides; morphology

## INTRODUCTION

Aromatic polyimides are, in general, difficult to process because of their lack of thermoplasticity. They are usually applied in the form of their precursors, the poly(amic acid) (PAA) in solution, followed by thermal imidization. The morphology of polyimides, notably the Kapton films produced by DuPont, has been examined by a number of investigations with different methods.<sup>1–7</sup> All of the results indicate the existence of molecular aggregations in the polyimide films, and conjugation occurs along the polyimide molecular chains.<sup>8–11</sup> It is generally accepted that the mechanical strength, thermal properties, and color of the aromatic polyimides are affected by the existence of electrons delocalized through conjugation along the polymer chains.

Solution casting of PAA followed by thermal imidization changes the reaction conditions from a solution to a solid state, depending on the rate of solvent vaporization. There have been some attempts to describe the morphology of polyimide.<sup>12–17</sup> In a previous article,<sup>18</sup> we reported the reactivities of PAA isomers in solution and in the solid state. This article describes the morphology of polyimide produced by imidization under different conditions.

## EXPERIMENTAL

### Preparation of polyimide pyromellitic dianhydride (PMDA)/oxydianiline (ODA)

PMDA was recrystallized from acetic anhydride and dried at 150°C *in vacuo*. ODA was purified by sublimation under reduced pressure. *N*-methyl-2-pyrrolidone (NMP) was dried over P<sub>2</sub>O<sub>5</sub> and distilled before use. The chemicals used were supplied by TCI (Tokyo, Japan), and the solvent was supplied by Merck (Darmstadt, Germany) and was reagent grade.

PAA was prepared by the dissolution of ODA in the NMP solvent followed by the addition of an equivalent amount of PMDA in several portions. The reaction was carried out at room temperature for 4 h. The solid content of the solution was about 20 wt %.

We carried out the thermal imidization of the PAA by (1) heating the solution in an Erlenmeyer flask to 400°C in an oven at a rate of 2°C/min and (2) precipitating PAA from methanol and then heating the solid PAA to 400°C in an oven at a rate of 2°C/min. The polyimide samples so obtained were designated as PI-1 and PI-2, respectively.

### Characterization of the polyimide

Wide-angle X-ray diffraction (WAXD) was performed with a Rigaku diffractometer (Tokyo, Japan) in a step scanning manner.

Solid-state <sup>13</sup>C-NMR spectra were recorded at 50.33 MHz with Me<sub>4</sub>Si as a reference standard on a Bruker MSL spectrometer (Karlsruhe, Germany). Cross-polarization/magic-angle spinning (CP-MAS) techniques were

Correspondence to: J.-W. Huang (hds63216@ms12.hinet.net).

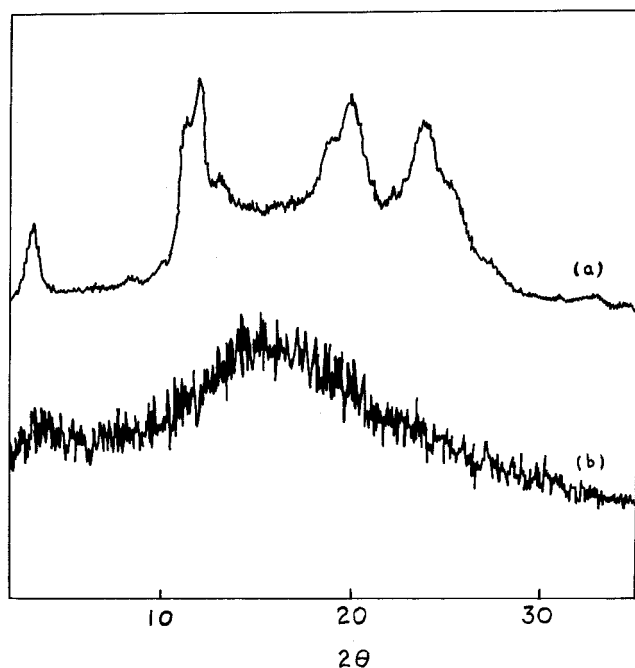


**Figure 1** WAXD spectra of polyimide PMDA/ODA: (a) PI-1 and (b) PI-2.

used to acquire the CP-MAS spectra with a spinning of 3.5 KHz, a contact time of 1 ms, and a repetition time of 1 s. Spin-lattice relaxation in the rotating frame was measured according to the method of Schaefer et al.<sup>19</sup>

IR spectra were recorded from KBr pellets. The spectral resolution of the Fourier transformation spectrometer (Bomen DA3002; Quebec, Canada) was  $0.5 \text{ cm}^{-1}$  for all of the spectra.

Electron paramagnetic resonance (EPR) was performed with a Bruker ER 200D spectrometer with 1-diphenyl-2-picrylhydrazyl (DPPH) as an internal standard.

Thermal properties of the polyimide were analyzed by a DuPont 910 differential scanning calorimeter and a DuPont 951 thermal gravimetric analyzer (New Castle, DE) at a scanning rate of  $10^\circ\text{C}/\text{min}$  under dry nitrogen. The samples used weighed about 10 mg.

## RESULTS AND DISCUSSION

The polyimide studied in this work was based on PMDA and ODA. This polymer has been investigated extensively, and a good deal of information is available in the literature for comparison. We obtained sample PI-1 by heating the PAA solution in an Erlenmeyer flask to  $400^\circ\text{C}$  into a powdered polyimide. Under these conditions, imidization took place to a large extent before the vaporization of the solvent. We obtained sample PI-2 by heating the PAA in the solid state. Both samples were characterized by WAXD,

$^{13}\text{C}$ -NMR spectroscopy, IR spectroscopy, EPR, and thermogravimetric analysis (TGA).

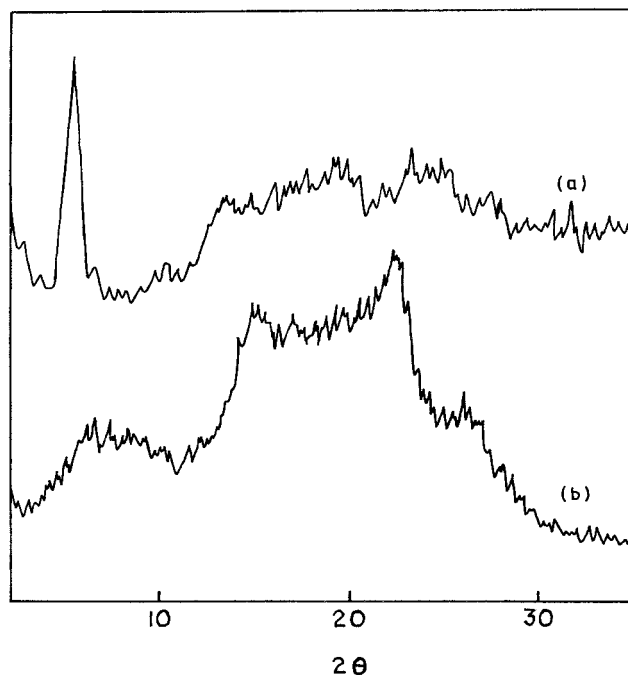
### WAXD analysis

Figure 1 shows the diffraction patterns of PI-1 and PI-2. When imidization was carried out in the solid state, the resulting polyimide (PI-2) showed the diffraction pattern of an amorphous material. However, when imidization was carried out in solution, the resulting polyimide (PI-1) gave the diffraction pattern of a crystalline material. Undoubtedly, the polymer chains had the mobility to arrange themselves into a crystalline form when imidization took place in solution.

A number of articles have described ordered polyimides in the form of films<sup>1-7</sup> and fibers.<sup>20-25</sup> For instance, the Kapton films based on PMDA/ODA (DuPont) have been shown to possess a significant degree of orientation of the molecules parallel to the film surface. However, the diffraction pattern of a Kapton film (Fig. 2) was by no means comparable to that of PI-1.

### CP-MAS $^{13}\text{C}$ -NMR spectral analysis

The chemical shift in  $^{13}\text{C}$ -NMR spectroscopy has long been recognized as a probe for assessing the electron structure of aromatic compounds. In these systems, shielding is governed primarily by the electron density at each carbon. Alger et al.<sup>26</sup> developed the fol-



**Figure 2** WAXD spectra of a Kapton film: (a) in-plane and (b) out-of-plane direction.

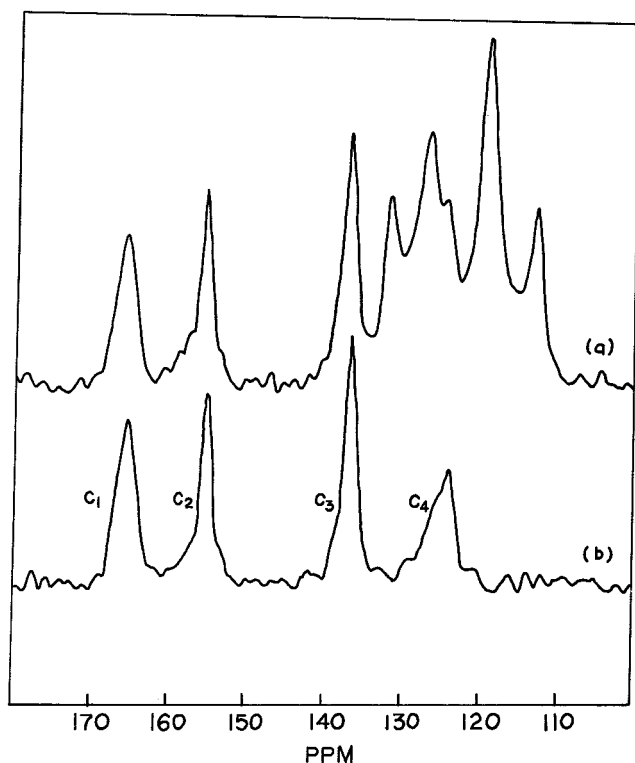


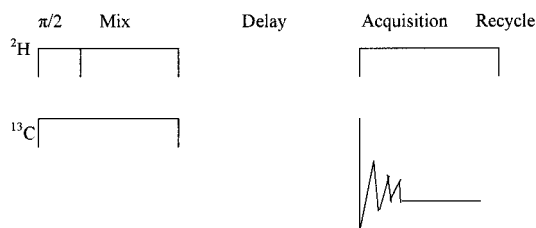
**Figure 3** CP-MAS  $^{13}\text{C}$ -NMR spectra of PI-1: (a) conventional and (b) dipolar dephased.

lowering relationship between the chemical shift ( $\delta$ ) and charge density:

$$\delta(^{13}\text{C}) = 100\Delta Q_{\pi} + 67\Delta Q_{\sigma} - 76\Delta P$$

where  $\Delta Q_{\pi}$ ,  $\Delta Q_{\sigma}$ , and  $\Delta P$  are the  $\pi$  charge, the  $\sigma$  charge, and the sum of the mobile bond orders (relative to the value of benzene), respectively.

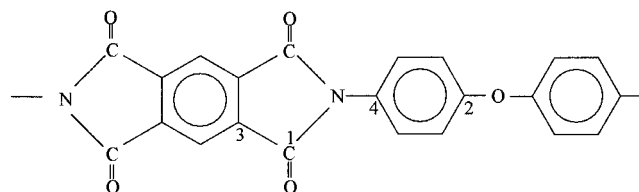
The CP-MAS  $^{13}\text{C}$ -NMR spectrum of PI-1, shown in Figure 3(a), was complex. The assignment of the signals was made with the aid of a dipolar dephasing experiment<sup>27</sup> as follows:



Before the Hartmann-Hahn match, a delay of 40  $\mu\text{s}$  was introduced in the  $^1\text{H}$  channel without spin locking. During this dephasing period, the relaxation of the protonated carbon atoms occurred. The signals of these carbon atoms were significantly attenuated in the dephasing spectrum, whereas those of the quaternary carbon atoms, which had no efficient relaxation

pathways, showed essentially no decrease in intensity [Fig. 3(b)].

The  $\text{C}_1$  and  $\text{C}_2$  signals in Figure 3(b) were assigned to the quaternary carbonyl carbon and the phenylene carbon bonded to oxygen, respectively.<sup>8</sup>  $\text{C}_3$  and  $\text{C}_4$  were attributed to the quaternary carbon atoms of the PMDA nuclei and the phenylene carbon bonded to nitrogen, respectively.



The assignments were based on the fact that the chemical shift of  $\text{C}_3$  was less affected than that of  $\text{C}_4$  from a series of polyimides derived from PMDA and different aromatic diamines. We expected the carbon atoms in the ordered state (e.g., in PI-1) to give rise to sharp, well-resolved peaks [Fig. 3(b)] because of the homogeneity of their local environment (with the assumption of no difference in bulk susceptibility), whereas we expected those in the amorphous state [e.g., in PI-2; Fig. 4(a,b)] to give rise to broadened peaks. This broadening effect is intrinsic to the sample structure and is not a result of instrumental limitations.<sup>28</sup> Ex-

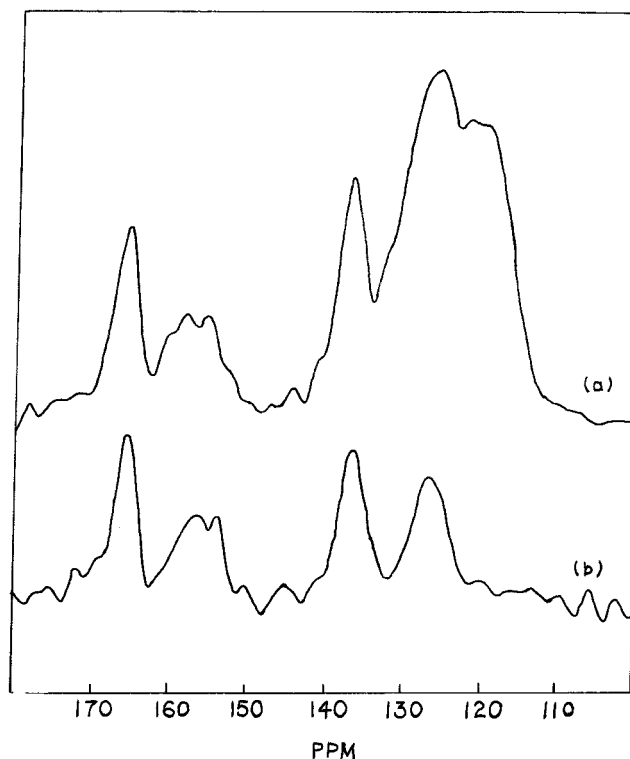


**Figure 4** CP-MAS  $^{13}\text{C}$ -NMR spectra of PI-2: (a) conventional and (b) dipolar dephased.

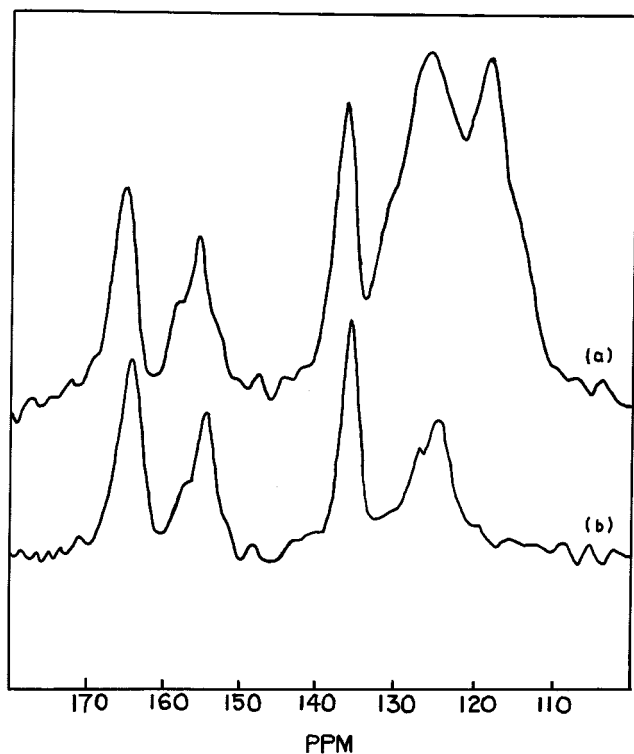
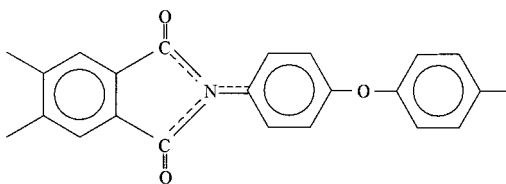


Figure 5 CP-MAS  $^{13}\text{C}$ -NMR spectra of a Kapton film: (a) conventional and (b) dipolar dephased.

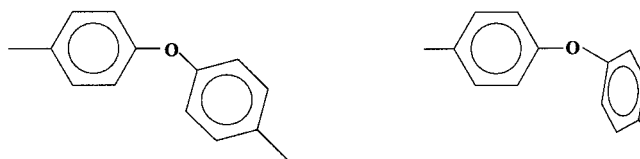
perimental evidence shows that the nitrogen atoms of the imide ring are coplanar. Conjugation between the benzene nuclei takes place through the imide linkage.<sup>10</sup>



In the  $^{13}\text{C}$ -NMR spectra of PI-1 and PI-2, the chemical shifts of both  $\text{C}_1$  and  $\text{C}_2$  were almost the same, at 165 and 125 ppm, respectively. The results indicate that the nitrogen atoms in both PI-1 and PI-2 were in an  $\text{sp}^2$  state.

The phenylene carbon bonded to oxygen ( $\text{C}_2$ ) in PI-1 gave a relatively sharp peak at 155 ppm, whereas that in PI-2 gave a broadened peak at 158 ppm in addition to the peak at 155 ppm [Fig. 3(b)]. To account for the conformational homogeneity of  $\text{C}_2$  in PI-1, we assumed that the two aromatic nuclei of the diphenyl ether moiety were coplanar and that conjugation between the aromatic nuclei occurred through the  $\text{C}-\text{O}-\text{C}$  linkage. The results from EPR, discussed later, seem to support this assumption. Thus, the broadened peak at 158 ppm was attributed to diphe-

nyl ether with two aromatic rings skewed to different degrees.

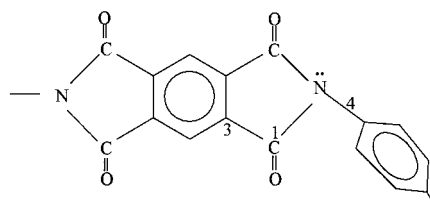


PI-1

PI-2

Conjugation between the aromatic nuclei could not occur through the  $\text{C}-\text{O}-\text{C}$  linkage when the two aromatic nuclei were out of plane. The signal shift downfield from 155 to 158 ppm was a result of a decreased electron density at  $\text{C}_2$  in PI-2.

It has been shown that an  $\text{sp}^2$  to  $\text{sp}^3$  transformation of the imide nitrogen takes place when stress is applied to the polymer chains. The two aromatic nuclei linked by the imide ring are then no longer coplanar.<sup>20</sup>



Once conjugation between the aromatic nuclei was disrupted, the electron density on the phenylene car-

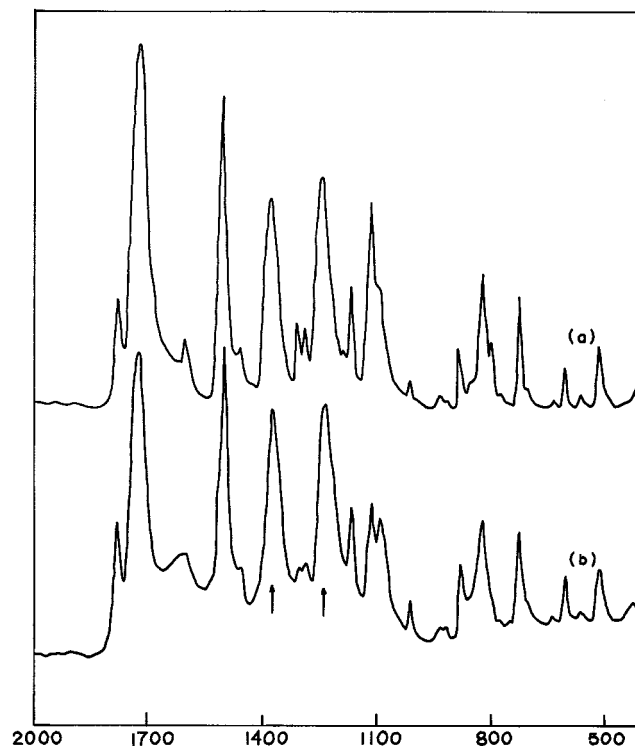


Figure 6 IR spectra of (a) PI-1 and (b) PI-2.

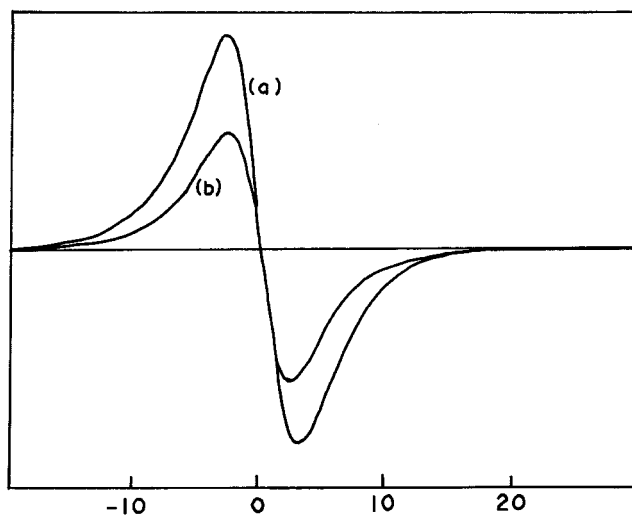


Figure 7 EPR spectra of (a) PI-1 and (b) PI-2.

bon ( $C_4$ ) was reduced, and the signal shifted downfield, for example, from 125 to 128 ppm.

For comparison, the  $^{13}\text{C}$ -NMR spectra of a Kapton film (shown in Fig. 5) was much smaller than that of the polyimide fiber, indicating that the polymer chains were under stress during film formation.

### IR spectral analysis

Figure 6 shows the IR spectra of PI-1 and PI-2. A notable difference between the spectra of these two samples was in the C—O—C stretching mode, which increased from  $1242\text{ cm}^{-1}$  in PI-2 to  $1249\text{ cm}^{-1}$  in PI-2 as a result of the increased conjugation accompanying crystallization.<sup>29-33</sup> The CN stretching mode of the polyimide was also affected by changes in the bond order of the ether linkage. The absorption peak of the CN stretching mode in PI-1 increased by  $4\text{ cm}^{-1}$  over that in PI-2.

### EPR spectral analysis

EPR spectroscopy records the transition between spin levels of molecular unpaired electrons in an external magnetic field. The area under the EPR signal is proportional to the number of unpaired spins in the sample. Figure 7 shows the EPR signals of PI-1 and PI-2 with DPPH used as an internal standard. The integrated area of PI-1 was twice that of PI-2, which indicated a higher density of mobile electrons through the polymer chain in PI-1. The  $g$  value in electron-spin resonance is the proportional constant in the following equation:<sup>34</sup>

$$h\nu = g\beta B$$

where  $h$  is Planck's constant,  $\nu$  is the fixed frequency of the microwave radiation,  $\beta$  is the Bohr magneton, and  $B$  is the magnitude of the static field at resonance. From the narrow symmetrical singlet EPR signals of PI-1 and PI-2, the  $g$  value was found to be 2.00415, approaching that of a free electron.

### Mobility of the molecular chains

The glass-transition temperatures of PI-1 and PI-2 were not detected by the differential scanning calorimeter up to  $500^\circ\text{C}$ . However, the microscopic chain motional behavior of the polymer chains was detected by measurement of the  $^{13}\text{C}$  spin-lattice relaxation in the rotating frame [ $T_{1\rho}(\text{C})$ ]. The average values of  $\langle T_{1\rho}(\text{C}) \rangle$  were determined by a least squares analysis of a plot of intensity versus contact time, as shown in Figure 8.

$T_{1\rho}(\text{C})$  reflects an average of the motional heterogeneity that exists for each individual carbon and, thereby, an average for the entire polymeric system.<sup>19,35</sup> The  $\langle T_{1\rho}(\text{C}) \rangle$  values of PI-1 and PI-2 were 103 and 43 ms, respectively. The polyimide chains had less motion in PI-1 than in PI-2 because of closer packing of the polymer chains on crystallization and an increased bond order through conjugation.

### TGA

As shown in the TGA of PI-1 and PI-2 in Figure 9, PI-1 showed a higher decomposition temperature than PI-2 by  $85^\circ\text{C}$ . In the case of carbon-chain polymers, thermal energy fluctuations localized inevitably at certain bonds, leading ultimately to bond ruptures. For polyimides, these fluctuations would be much less as a result of their rapid distribution over all of the link-

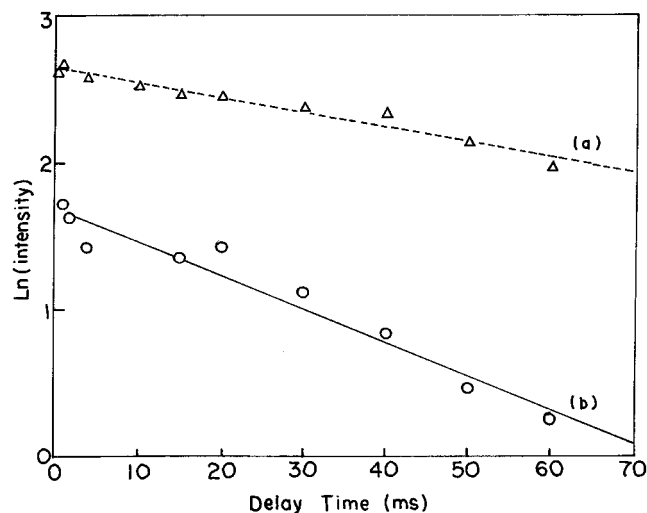


Figure 8 Rotating frame relaxation time of (a) PI-1 and (b) PI-2.

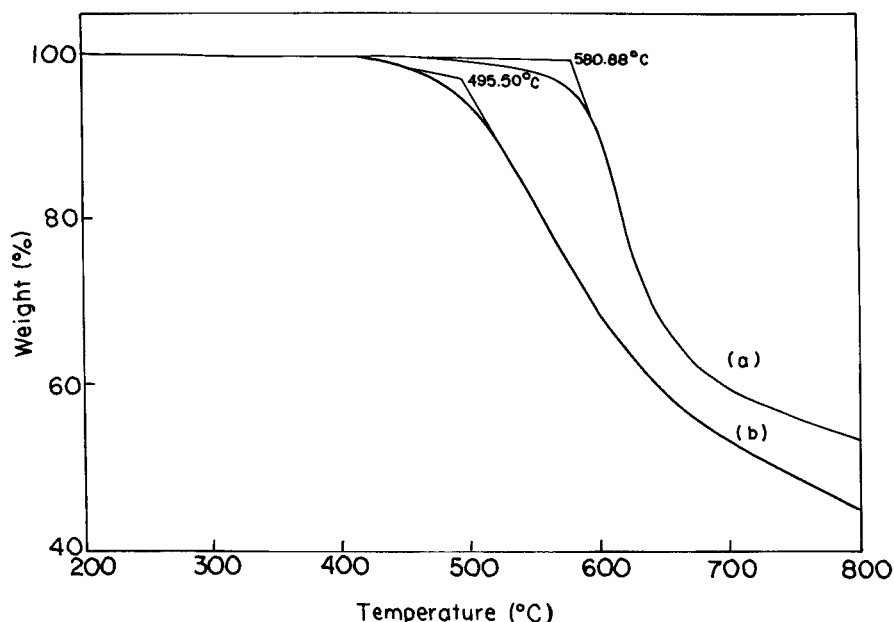


Figure 9 TGA of (a) PI-1 and (b) PI-2.

ages and atoms through the mobile electrons.<sup>36</sup> PI-1 had a better thermal stability than PI-2 because of its higher degree of conjugation along the polymer chain.

## References

- Isoda, S.; Shimada, H.; Kochi, M.; Kambe, H. *J Polym Sci Polym Phys Ed* 1981, 19, 1293.
- Russell, T. P.; Gugyer, H.; Swalen, J. D. *J Polym Sci Polym Phys Ed* 1983, 21, 1745.
- Russell, T. P. *Polym Sci Ed* 1984, 22, 1105.
- Takahashi, N.; Yoon, D. Y.; Parrish, W. *Macromolecules* 1984, 17, 2583.
- Wachsmann, E. D.; Frank, C. W. *Polymer* 1988, 29, 1191.
- Pryde, C. A. *J Polym Sci Part A: Polym Chem* 1989, 27, 711.
- Lebedev, G. A. *Vysokomol Soedin A* 1975, 17, 1164.
- Havens, J. R.; Ishida, H.; Koenig, J. L. *Macromolecules* 1981, 14, 1327.
- Brikson, B. R.; Frelmanis, Y. F. *Vysokomol Soedin A* 1970, 12, 69.
- Gordina, T. A.; Kotov, B. V.; Kolniov, O. V.; Pravednikov, A. N. *Vysokomol Soedin B* 1973, 15, 378.
- Kotov, B. V.; Gordina, T. A.; Voischev, V. S.; Kolinov, O. V.; Pravednikov, A. N. *Vysokomol Soedin A* 1977, 19, 614.
- Goel, R. N.; Hepworth, A.; Deopura, B. L.; Varma, I. K.; Varma, D. S. *J Appl Polym Sci* 1979, 23, 3541.
- Jennings, R. M.; Farris, R. J. *J Polym Sci Part B: Polym Phys* 1994, 8, 1457.
- Brillhart, M. V.; Cheng, Y. Y.; Nagarkart, P.; Cebe, P. *Polymer* 1997, 12, 3059.
- Basset, F.; Lefrant, A.; Pascal, T.; Gallot, B.; Sillion, B. *Polym Adv Technol* 1998, 9, 202.
- Dorsey, K. D.; Desai, P.; Abhiraman, A. S.; Hinkley, J. A.; St. Clair, T. L. *J Appl Polym Sci* 1999, 7, 1215.
- Kang, J. W.; Choi, K.; Jo, W. H.; Hsu, S. L. *Polymer* 1998, 39, 7079.
- Chu, N. J.; Huang, J. W. *Polym J* 1990, 22, 725.
- Schaefer, J.; Stejskal, E. O.; Buchdahl, R. *Macromolecules* 1977, 10, 384.
- Cherkasov, A. N.; Vitovakaya, M. G.; Bushin, S. V. *Vysokomol Soedin A* 1976, 18, 1628.
- Tuichiev, S.; Korzhavin, L. N.; Prokhov, O. Y.; Ginzburg, B. M.; Frenkel, S. Y. *Vysokomol Soedin A* 1971, 13, 1463.
- Kazaryan, L. G.; Tsvankin, D. Y.; Ginzburg, B. M.; Tuichiev, S.; Korzhavin, L. N.; Frenkel, S. Y. *Vysokomol Soedin A* 1972, 14, 1199.
- Goel, R. N.; Varma, I. K.; Varma, D. S. *J Appl Polym Sci* 1979, 24, 1061.
- Kaneda, T.; Katsura, T.; Nakagawa, K.; Makino, H.; Horio, M. *J Appl Sci* 1986, 32, 3151.
- Dorogy, W. E., Jr.; St. Clair, A. K. *J Appl Polym Sci* 1991, 43, 501.
- Alger, T. D.; Grant, D. M.; Paul, E. G. *J Am Chem Soc* 1966, 88, 5397.
- Opella, S. J.; Frey, M. H. *J Am Chem Soc* 1979, 101, 5854.
- Sefcik, M. D.; Schaffer, J.; Stejskal, E. O.; Mckay, R. A. *Macromolecules* 1980, 13, 1132.
- Wellinghof, S. T.; Ishida, H.; Koenig, J. L.; Baer, E. *Macromolecules* 1980, 13, 834.
- Ishida, H.; Wellinghof, S. T.; Baer, E.; Koenig, J. L. *Macromolecules* 1980, 13, 826.
- Garrigou-Lagrange, C.; Horak, M.; Khanna, R. K.; Lippincot, E. R. *Collect Czech Chem Commun* 1970, 35, 3230.
- Katritzky, A. R.; Pimzelli, R. F.; Topsom, R. D. *Tetrahedron* 1972, 28, 3441.
- Horak, M.; Josefi, R. *Collect Czech Chem Commun* 1972, 39, 3209.
- Carrington, A.; McLachlan, A. D. *Introduction to Magnetic Resonance*; Harper & Row: New York, 1967.
- Schaefer, J.; Stejskal, E. O.; Steger, T. R.; Sefcik, M. D.; Mckay, R. A. *Macromolecules* 1980, 13, 1121.
- Fainshtein, E. B.; Lushcheikin, G. A.; Igonin, L. A. *Vysokomol Soedin A* 1974, 16, 1677.